Solvent Fuming Dual-Responsive Switching of Both Wettability and Solid-State Luminescence in Silole Film

Liping Heng, Yongqiang Dong, Jin Zhai,* Benzhong Tang,* and Lei Jiang

Beijing National Laboratory for Molecular Sciences (BNLMS), Center for Molecular Science, Institute of Chemistry, Chinese Academy of Sciences, Beijing 100080, China, Departments of Chemistry, Hong Kong University of Science and Technology, Clear Water Bay, Kowloon, Hong Kong, P. R. China, and Graduate School of Chinese Academic of Science, Beijing 100864, China

Received September 18, 2007. In Final Form: November 4, 2007

A multiresponsive switcher on both wettability and solid-state luminescence has great application potentials in novel smart devices. In this paper, a silole molecule of 1,2,3,4,5-hexaphenylsilole (HPS) was chosen to prepare thin films by spin-coating, and a solvent fuming dual-responsive switcher combining photoluminescent behavior and wettability was successfully achieved by changing the mode of solid-state molecular packing. This study suggests that HPS and other silole derivatives have a promising future for use in dual- and multifunctional switches in new technological applications.

Introduction

Stimuli-responsive materials,[1] which can sense inner and/or outer stimuli, then analyze, dispose, and judge in order to adopt an approach for the appropriate responses, have been developed rapidly as novel composite materials due to their extensive use in fields such as "smart" surface coating,[2] drug delivery,[3] chemical and biological sensing,[4] catalysis,[5] color-tunable crystals,[6] and information storage.[7] Recently, several responsive smart interfacial materials that can switch between hydrophilicity and hydrophobicity,[8] fluorescence on and off,[9] and other physical and chemical properties[10] have been reported. However, all of these switches are one-way systems; to the best of our knowledge, the development of two-way responsive materials, such as those capable of reversibly switching between different properties, is still at its infancy, and continues to be a challenge to modern material science. Very recently, nanostructure tungsten oxide films with wettability and photochromic dual-responsive properties were successfully prepared by a facile electrochemical deposition method,[11] providing a good example for the fabrication of two-way responsive materials. In this paper, we replaced inorganic oxide materials with organic small molecules achieving a dual-responsive switcher on both wettability and solid-state luminescence by adjusting the molecular packing mode.

As is known, silole is an important class of molecules that exhibit unusual aggregation-induced emission (AIE) properties.[12] They are weakly luminescent or practically nonluminescent in solution, but become highly emissive when aggregated into nanoclusters or thin films. Furthermore, their emission maximums can be controlled by their aggregation morphology. It shows that a silole molecule of 1,2,3,4,5-hexaphenylsilole (HPS) practically emits at around 500 nm in the form of amorphous bulk solid, while it shows 465 nm luminescence upon formation of crystal bulk solid.[13] Due to this phenomenon, HPS was chosen to prepare thin films by spin-coating, and a solvent fuming dual-responsive switcher combining photoluminescent behavior and wettability was successfully achieved, which would lead to future uses for HPS in novel smart devices such as intelligent microfluidic switch, information storage, field emission, optical modulation, electroluminescence, photovoltaic, vapor-sensor, and immunoassay systems.

* Tel. & Fax: (+86) 10-82627566. Email: zhaijin@iccas.ac.cn.

(1) (a) Gil, E. S.; Hudson, S. M. *Prog. Polym. Sci.* **2004**, *29*, 1173; (b) Jeong, B.; Gutowska, A. *Trends Biotechnol* **2002**, *20*, 305; (c) Kikuchi, A.; Okano, T. *Prog. Polym. Sci.* **2002**, *27*, 1165; (d) Hoffman, A. S. et al. *J. Biomed. Mater. Res.* **2000**, *52*, 577; (e) Galaev, L. Y.; Mattiasson, B. *Trends Biotechnol.* **2000**, *17*, 335.

(2) (a) Russell, T. P. *Science* **2002**, *297*, 964; (b) Nath, N.; Chilkoti, A. *Adv. Mater.* **2002**, *14*, 1243.

(3) Jeong, B.; Kim, S. W.; Bae, Y. H. *Adv. Drug Delivery Rev.* **2002**, *54*, 37.

(4) (a) Hu, Z. B.; Chen, Y. Y.; Wang, C. J.; Zheng, Y. D.; Li, Y. *Nature (London)* **1998**, *393*, 149; (b) Van der Linden, H.; Herber, S.; Olthuis, W. *Sens. Mater.* **2002**, *14*, 129.

(5) Bergbreiter, D. E.; Case, B. L.; Liu, Y. S.; Waraway, J. W. *Macromolecules* **1998**, *31*, 6053.

(6) Debord, J. D.; Eustis, S.; Debord, S. B.; Lofye, M. T.; Lyon, L. A. *Adv. Mater.* **2002**, *14*, 658.

(7) (a) Yuan, W. F.; Sun, L.; Tang, H. H.; Wen, Y. Q.; Jiang, G. Y.; Huang, W.; Jiang, L.; Song, Y. L.; Tian, H.; Zhu, D. B. *Adv. Mater.* **2005**, *17*, 156; (b) Jiang, G. Y.; Song, Y. L.; Wen, Y. Q.; Yuan, W. F.; Wu, H. M.; Yang, Z.; Xia, A. D.; Feng, M.; Du, S. X.; Gao, H. J.; Jiang, L.; Zhu, D. B. *ChemPhysChem* **2005**, *6*, 1478.

(8) (a) Zhu, W. Q.; Feng, X. J.; Feng, L.; Jiang, L. *Chem. Commun.* **2006**, *26*, 2753; (b) Feng, X. J.; Feng, L.; Jin, M. H.; Zhai, J.; Jiang, L.; Zhu, D. B. *J. Am. Chem. Soc.* **2004**, *126*, 62; (c) Feng, X. J.; Zhai, J.; Jiang, L. *Angew. Chem., Int. Ed.* **2005**, *44*, 5115; (d) Sun, T. L.; Wang, G. J.; Feng, L.; Liu, B. Q.; Ma, Y. M.; Jiang, L.; Zhu, D. B. *Angew. Chem., Int. Ed.* **2004**, *43*, 357.

(9) Mutai, T.; Satou, H.; Araki, K. *Nat. Mater.* **2005**, *4*, 685.

(10) (a) Webber, G. B.; Wanless, E. J.; Armes, S. P.; Tang, Y. Q.; Li, Y. T.; Biggs, S. *Adv. Mater.* **2004**, *16*, 1794; (b) Li, C. M.; Madsen, J.; Armes, S. P.; Lewis, A. L. *Angew. Chem., Int. Ed.* **2006**, *45*, 3510; (c) Chen, Y. L.; Gautrot, J. E.; Zhu, X. X. *Langmuir* **2007**, *23*, 1047.

(11) Wang, S. T.; Feng, X. J.; Yao, J. N.; Jiang, L. *Angew. Chem., Int. Ed.* **2006**, *45*, 1264.

(12) (a) Luo, J. D.; Xie, Z. L.; Lam, J. W. Y.; Cheng, L.; Chen, H. Y.; Qiu, C. F.; Kwok, H. S.; Zhan, X. W.; Liu, Y. Q.; Zhu, D. B.; Tang, B. Z. *Chem. Commun.* **2001**, *18*, 1740; (b) Bhongale, C. J.; Chang, C. W.; Diau, E. W. G.; Hsu, C. S.; Dong, Y. Q.; Tang, B. Z. *Chem. Phys. Lett.* **2006**, *419*, 444; (c) Yu, G.; Yin, S. W.; Liu, Y. Q.; Chen, J. S.; Xu, X. J.; Sun, X. B.; Ma, D. G.; Zhan, X. W.; Peng, Q.; Shuai, Z. G.; Tang, B. Z.; Zhu, D. B.; Fang, W. H.; Luo, Y. *J. Am. Chem. Soc.* **2005**, *127*, 6335; (d) Ren, Y.; Lam, J. W. Y.; Dong, Y. Q.; Tang, B. Z.; Wong, K. S. *J. Phys. Chem. B* **2005**, *109*, 1135.

(13) (a) Chen, J. W.; Xu, B.; Yang, K. X.; Cao, Y.; Sung, H. H. Y.; Williams, I. D.; Tang, B. Z. *J. Phys. Chem. B* **2005**, *109*, 17086; (b) Dong, Y. Q.; Lam, J. W. Y.; Li, Z.; Qin, A. J.; Tong, H.; Dong, Y. P.; Feng, X. D.; Tang, B. Z. *J. Inorg. Organomet. Polym.* **2005**, *15*, 287; (c) Li, Z.; Dong, Y. Q.; Mi, B.; Tang, Y. H.; Häussler, M.; Tong, H.; Dong, Y. P.; Lam, J. W. Y.; Ren, Y.; Sung, H. H. Y.; Wong, K. S.; Gao, P.; Williams, I. D.; Kwok, K. S.; Tang, B. Z. *J. Phys. Chem. B* **2005**, *109*, 10061.

10.1021/la702888v CCC: $40.75 © 2008 American Chemical Society
Published on Web 01/19/2008

Scheme 1 [a]

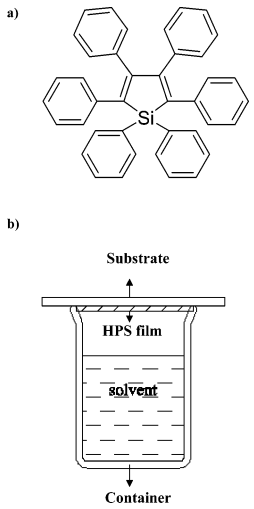

[a] (a) Chemical structure of HPS; (b) the equipment for solvent vapor fuming.

Experimental Section

Sample Preparation. 1,2,3,4,5-hexaphenylsilole (HPS) was synthesized according to the literature,[14] and its chemical structure is shown in Scheme 1a. ^{1}H NMR (300 MHz, $CDCl_3$): δ 7.68 (m, 4H), 7.43 (m, 6H), 7.20−6.85 (m, 20H). FT-IR (KBr): 3055, 3024, 1597, 1485, 1441, 1429, 1298, 1111, 1074, 1027, 790, 764, 741, 713, 697, 509 cm^{-1}. MS (EI): *m*/*z* 538 (called for $C_{40}H_{30}Si$ 538.76). Anal. Calcd for $C_{40}H_{30}Si$: C, 89.18; H, 5.61. Found: C, 89.46; H, 5.56%.

HPS was dissolved in purified tetrahydrofuran (THF) to form saturated solution. The solution was spin-coated onto the freshly cleaned glass at 1000 rpm for 15 s, and HPS film A was obtained. Then, film A was exposed to ethanol solvent vapors by placing a small open container with solvent beneath the film and keeping at room temperature for 10 min; HPS film B was obtained. The equipment for solvent vapor fuming is given in Scheme 1b. In the reversible step, film B was solvent vapor annealed by alternating ethanol with toluene at room temperature for 13 min, and film A was obtained reversibly.

Sample Characterization. Morphology of the films was investigated using a JEOL JSM-6700F scanning electron microscopy (SEM) at 3.0 kV. UV−vis absorbance spectra were carried out using a Hitachi U-4100 spectrometer, and the fluorescent spectra were measured by a Hitachi F-4500 fluorescence spectrophotometer.

Contact angle (CA) was measured on a Dataphysics OCA20 CA system at ambient temperature. The average CA value was obtained by measuring more than five different positions for the same sample.

X-ray diffraction (XRD) measurements were performed by using a Rigaku X-ray diffractometer (D/max-2400) with an X-ray source of Cu K_α (λ = 0.154 06 nm) at 40 kV and 120 mA, at a scan rate of 0.02° (2θ) per 0.12 s.

Results and Discussion

Figure 1a−d shows the typical field emission scanning electron microscopy (FE-SEM) images of the as-prepared HPS films. It can be seen clearly that film A is smooth and featureless (Figure 1a), since they are kinetically trapped in disordered state during the spin-coating process. The cross-sectional image (Figure 1c) confirms that film A is solid with the total thickness of 4.5 μm. Nanosheets and nanorods with the thickness 100−400 nm, width 3−10 μm, and length of several tens of micrometers can be observed on the surface of film B (Figure 1b). For comparison,

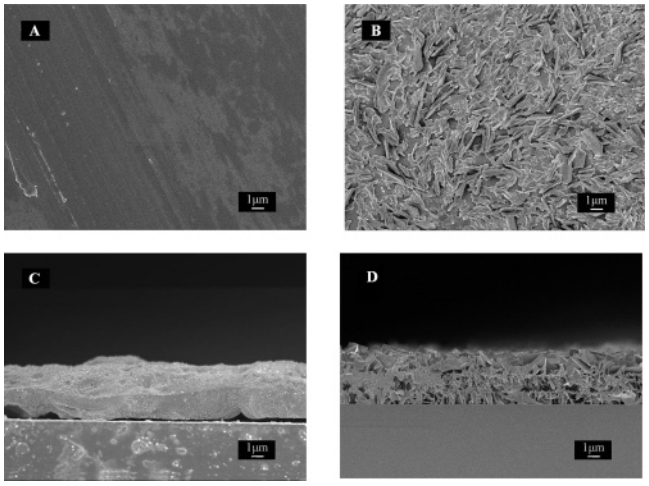

Figure 1. Top view SEM images of film A (a) and film B (b). As shown, film A is smooth and featureless, while film B is composed of nanosheets and nanorods of HPS. Side view SEM images of film A (c) and film B (d) The thickness of film A is ca. 4.5 μm, and that for film B is ca. 5.0 μm.

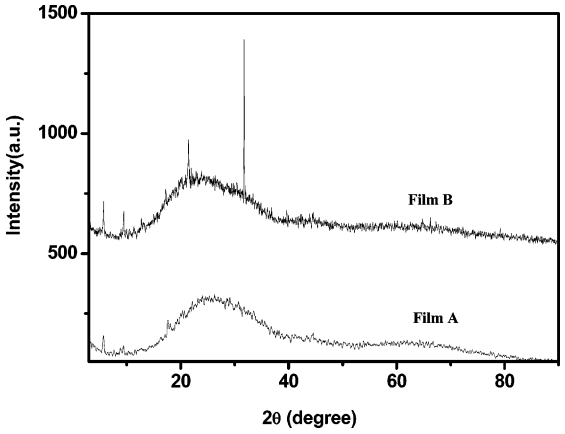

Figure 2. XRD patterns of film A and film B. Film A was confirmed to be amorphous from the absence of any specific patterns in XRD, while film B exhibited sharp diffraction peaks, indicating its crystalline state of HPS.

the cross-sectional SEM image of film B is shown in Figure 1d, and the film thickness is measured as ca. 5.0 μm. The morphology of film B could be changed back to that of film A when film B was exposed into toluene vapor.

By investigation by X-ray diffraction (XRD), film A is confirmed to be amorphous from the absence of any specific patterns in XRD, while film B exhibits many sharp diffraction peaks at low angles and small diffraction peaks at high angles (Figure 2). This result indicates that ethanol solvent vapor annealing is favored for regular arrangement of the HPS molecule and convenient for the formation of microcrystals. Toluene vapor exposure brings the disappearance of sharp diffraction peaks once again, and amorphous HPS film is achieved.

As shown in Figure 3, the UV−vis spectra show that the absorption peak of HPS in both film A and film B appear in the same region around 370 nm with a similar shape, suggesting a similar photoexcitation process in both solid states.

Since HPS is an excellent fluorescence material, its photoluminescence behavior was studied at once. From Figure 4, it can be clearly seen that, upon 370 nm light excitation, film A emits a green light with the peak at 494 nm, while film B emits a blue light with the peak at 465 nm. The photos of film A and film B, which are inset in Figure 4, were taken under illumination

(14) (a) Tang, B. Z.; Zhan, X.; Yu, G.; Lee, P. P. S.; Liu, Y.; Zhu, D. *J. Mater. Chem.* **2001**, *11*, 2974; (b) Chen, J.; Law, C. C. W.; Lam, J. W. Y.; Dong, Y. P.; Lo, S. M. F.; Williams, I. D.; Zhu, D.; Tang, B. Z. *Chem. Mater.* **2003**, *15*, 1535.

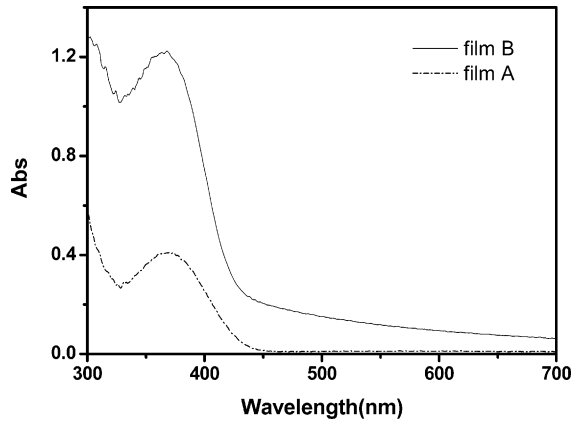

Figure 3. UV absorption spectra of film A and film B, showing no difference of absorption peaks at 370 nm for film A and film B.

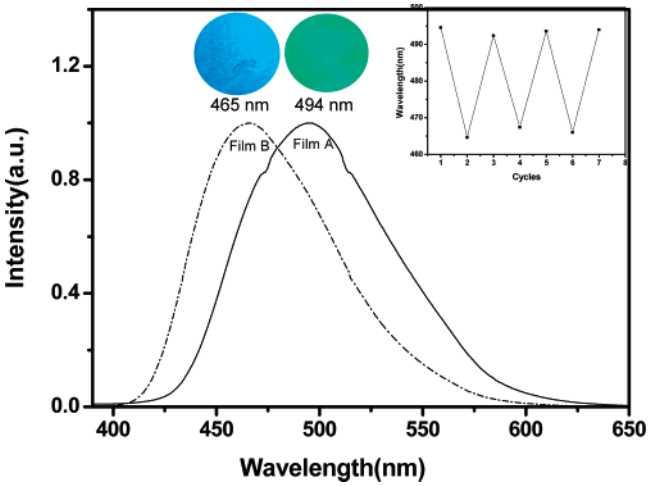

Figure 4. Normalized photoluminescence spectra of film A and film B excited by the light of 370 nm. Inset: (Left) photographs of the HPS films at different aggregations taken under illumination of a UV light (325 nm). (Right) reversible luminescence transition of the as-prepared HPS films against the number of ethanol−toluene vapor cycles starting from film A.

of a UV light (325 nm). Interestingly, the results indicate that a solvent vapor fuming reversible switch between the green light and the blue light luminescent is realized by controlling the aggregation morphology of HPS. The green light luminescent film A turns to be blue light luminescent film B through ethanol vapor fuming and returns to the green light luminescent film A again by subsequent toluene vapor fuming. The repeated cycles shown in the inset of Figure 4 demonstrate that luminescence switching is reproducible without any sign of degradation or chemical reaction of the HPS molecules.

The surface wettability of the as-prepared HPS films was evaluated by water contact angle (CA) measurements. The CA on film A is 97.0 ± 1.5° (Figure 5a), thus indicating that the surface is hydrophobic. After film A is exposed in ethanol vapor, the water droplet shrinks on film B and results in a CA of 136.3 ± 1.6° (Figure 5a), showing that film B becomes more hydrophobic than film A. After keeping film B in toluene vapor for 13 min, the surface of film B thus returns to its initial state and the CA of the film converts to the original value. This cycle was repeated several times, and a good reversibility of surface wettability was observed (Figure 5b).

As is known, surface wettability is determined by surface roughness and surface free energy.[15−18] As cast, HPS film A shows hydrophobicity (CA = 97.0 ± 1.5°) because of its chemical composition having no hydrophilic groups. By exposing film A to ethanol vapor, the crystalline solid film B can be formed. It was proposed that the water droplet may shrink on the crystal surface with the contact angle of 136.3 ± 1.6° because of the formation of the nanostructures. From the SEM image (Figure 1b), it can be seen that the nanobelts and nanorods on film B are formed and separated from each other. Therefore, an air pocket[18] at the interface between water and the nanostructures of film B can be formed. Theoretically, eq 1 formulated by Cassie and Baxter[18b] describes the contact angle at a composite surface.

$$\cos \theta_f = f_s \cos \theta_w - f_v \quad (1)$$

In this case, θ_f and θ_w are the contact angles on film B and film A, respectively, f_s and f_v are the fractional interfacial areas of the HPS nanorods and the air in the troughs between individual nanorods, respectively (i.e., $f_s + f_v = 1$). It is easy to deduce from eq 1 that an increase in f_v will lead to an increase in θ_f. According to eq 1, the value of f_v of HPS film B can be calculated to be 0.681, indicating that the air trapped in the films enhances the hydrophobicity of the surface.[18] Moreover, the HPS crystal state is more stable than its amorphous state,[13] so the crystal state has the lower surface energy, which is responsible for the increasing of the CA on the crystal thin film at the same time.

In fact, the unusual molecular packing in the two kinds of solid thin films is responsible for these solvent fuming dual reversible switches. The as-cast HPS film A is kinetically trapped in the disordered state due to the spin-coating process. When placed into ethanol vapor, the solvent vapor may be condensed and hence form thin liquid layers, which could dissolve the HPS molecules. Considering the low solubility of HPS molecules in ethanol, the adsorption of solvent molecules during solvent-vapor exposure is suggested to result in a saturated solution on film A.[19] Adsorbed solvent molecules may cause a relaxation of a metastable crystal lattice or an increase in molecular motility at the surface of an amorphous thin film, thereby enabling nucleation of a stable crystalline form. If the ethanol vapor is altered with toluene vapor, HPS molecules have no enough time to arrange themselves, and an amorphous solid state can be formed because of the higher solubility of HPS in toluene and faster vaporize speed.

In order to understand the extension of the solvent vapor annealing, other annealing experiments with two series of solvents (one is ethanol-like, the other is toluene-like) for HPS molecules were also carried out. As to the ethanol-like solvent, acetone and methanol vapor annealing occur much more quickly than that for ethanol vapor (with periods of 5 and 8 min, respectively), but annealing with isopropyl alcohol occurs more slowly (11 min) (as shown in Figure 6a). After annealing, the emissive maximal wavelengths are at ca. 465 nm, while the CA is ca. 135° (except for acetone) (Supporting Information S1a), indicating the crystal morphology of HPS film (film B). The crystal microstructures can be observed in Figure 7b,d,f, while nanobelts or nanorods were formed on the solid HPS crystal films. When annealed in toluene-like solvent vapors (toluene, benzene, chlorobenzene, tetrahydrofuran), the responsive times of tetrahydrofuran and benzene are faster than that of toluene (with periods of 3 and 5 min, respectively), while that for chlorobenzene

(15) Barthlott, W.; Neinhuis, C. *Planta* **1997**, *202*, 1.
(16) Sun, T. L.; Feng, L.; Gao, X. F.; Jiang, L. *Acc. Chem. Res.* **2005**, *38*, 644.
(17) Feng, X. J; Jiang, L. *Adv. Mater.* **2006**, *18*, 3063.
(18) (a) Wenzel, R. N. *Ind. Eng. Chem.* **1936**, *28*, 988; (b) Cassie, A. B. D.; Baxter, S.; *Trans. Faraday Soc.* **1944**, *40*, 546.
(19) (a) John, C. C.; Eric, J. C. O.; David, M. A.; Josef, K.; Arie, Z.; Brian, A. G.; Paul, F. B. *J. Phys. Chem. B* **1998**, *102*, 4516; (b) Debra, J. M.; Mark, E. T.; Henry, I. S.; Vladimir, B. *Org. Electron.* **2005**, *6*, 211.

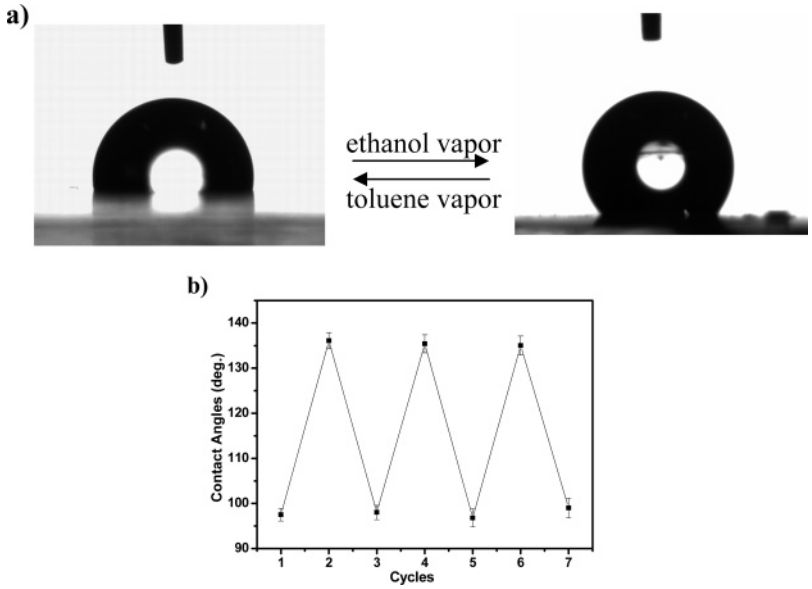

Figure 5. (a) Photographs of water droplet shape on film A with a CA of 97.0 ± 1.5° and on film B with a CA of 136.3 ± 1.6°. (b) Reversible contact angle transition of the as-prepared HPS films against the number of ethanol−toluene vapor cycles starting from film A.

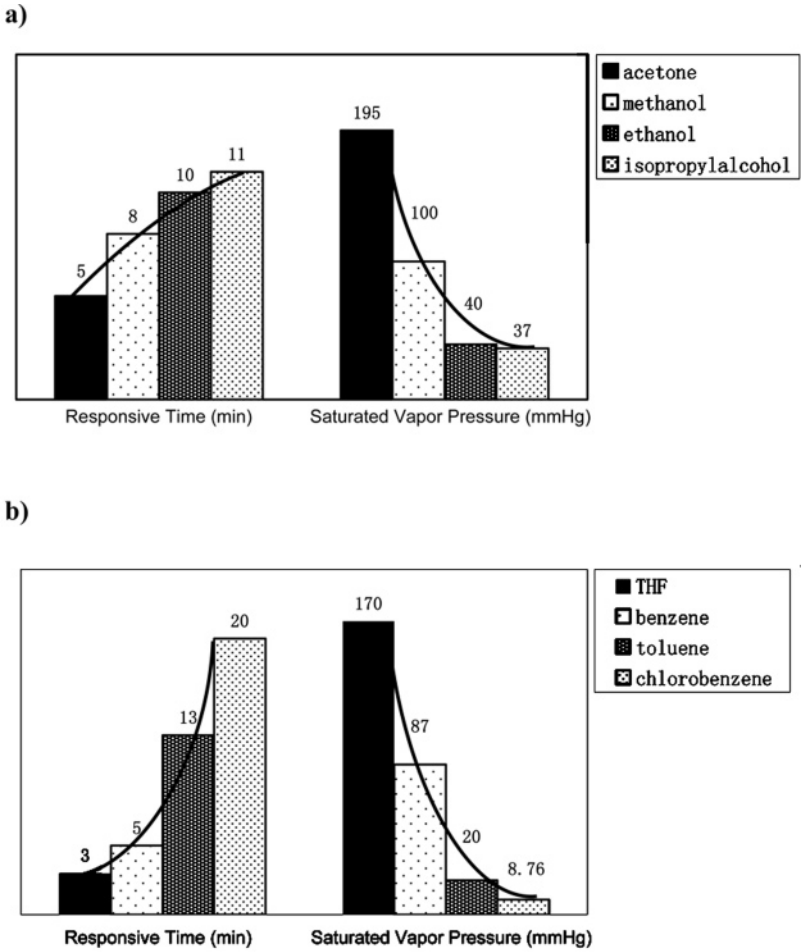

Figure 6. (a) Graph of ethanol-like solvent vapors responsive time and solvent saturated vapor pressure. (b) Graph of toluene-like solvent vapors responsive time and solvent saturated vapor pressure. The above graphs indicate that the responsive time increases with the decrease of the solvent saturated vapor pressure, which was determined by the speed of solvent volatilization.

is relatively slower (20 min) (as shown in Figure 6b). The emissive maximal wavelengths are at ca. 495 nm, while the CA is ca. 97° (Supporting Information S1b), indicating that the crystal morphology of film B changed to the amorphous state of film A. The morphologies were shown in the SEM images in Figure 7c,e,g, respectively, indicating smooth and featureless amorphous HPS films. Due to this difference of the microstructure in the two kinds of HPS thin films, these two kinds of HPS thin films by two series of solvent vapor annealing have different contact angle data and emissive maximal wavelength. All these experiments show that the solvent fuming dual-responsive switch has wide extension into future applications. By the way, for the two series

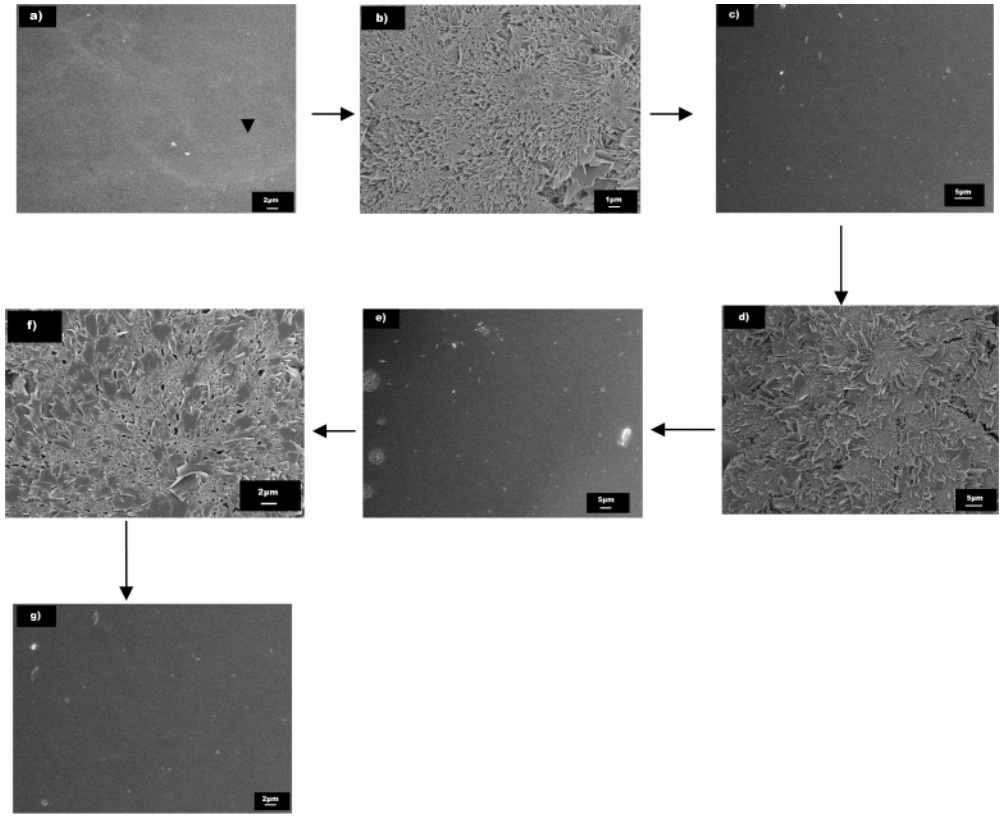

Figure 7. SEM images of (a) smooth film, (b) film after methanol vapor annealing; the nanobelts and nanorods are formed on the crystal solid film; (c) after benzene vapor annealing; nanobelts and nanorods disappeared, and amorphous HPS film is achieved; (d) after isopropyl alcohol vapor annealing; nanobelts and nanorods occur on the HPS film again; (e) after chlorobenzene vapor annealing; smooth surface is obtained; (f) after acetone vapor annealing; nanobelts and nanorods appearing on the HPS film once again; and (g) after tetrahydrofuran vapor annealing; the morphology changes back to that of featureless HPS.

of solvents, it can be seen that the responsive time increases with the decrease of the saturated vapor pressure, which determines the speed of solvent volatilization. The saturated vapor pressure of solvents is larger, the volatilization speed of solvents is faster, and hence the responsive time is shorter.

Conclusion

In conclusion, HPS films with solid-state luminescence and wettability dual-responsive properties have been prepared by the facile spin-coated process. A reversible solid-state luminescence conversion, which is accompanied by wettability, can be realized for this HPS material by alternating different solvent vapor exposing. The solid-state luminescence and wettability interconversion are coherent in nature and are due to changes in the mode of solid-state molecular packing. Because alteration of the mode of molecular packing does not require chemical reactions, the present findings would open the way for organic luminescent switches that can be controlled by external stimuli. This study suggests that HPS and other siloles have a promising future for use in dual- and multifunctional switches in new technological applications such as smart functional windows, bioanalysis, sensitive detection, and the potential for two-dimensional imaging.

Acknowledgment. The work was supported by the National Natural Science Foundation of China (No. 20573120, No. 50533030, No. 20773142), 973 program (No. 2006CB806200, 2006CB932100, 2007CB63403) and the Competitive Earmarked Research Grant of the Research Grants Council of the Hong Kong Special Administrative Region, China.

Supporting Information Available: Additional information as indicated in the text. This material is available free of charge via the Internet at http://pubs.acs.org.

LA702888V